First results of heat transfer measurements in a new water-cooled combustor on the Mascotte facility

G. Ordonneau, P. Hervat, L. Vingert, S. Petitot and B. Pouffary***
** Onera – The French Aerospace Lab.*
F-92322 Châtillon, France
***Cnes – Launcher Directorate*
F-91300 Evry, France

Abstract
The acceptance tests of a new water-cooled combustion chamber, which was developed for Onera's Mascotte test facility in cooperation with the CNES Launchers Directorate, are reported. The first goal of this device is to provide longer operation times in hot gas conditions, representative of rocket engines main combustion chambers, for CARS or PIV experiments. The walls are equipped with many thermocouples, used to investigate heat transfer in a wide range of operating pressures (up to 7 MPa) and mixture ratios (up to 7.5) in order to validate the assumptions retained for the design. The hardware, the measurements techniques and results are described.

1. Introduction
Detailed experimental studies of cryogenic propellant combustion, in well controlled and nevertheless representative operating conditions, are needed to optimize the design of high performance liquid rocket engines. Therefore a research test facility called Mascotte was built up by Onera in the mid-90's, to investigate elementary processes that are involved in the combustion of liquid oxygen and gaseous hydrogen near the exit of a single coaxial injector. During the last decade, several improvements have been made: the use of methane instead of hydrogen [1], the operation of multi-injector chambers [2] and the analysis of separated flow in an over-expanded nozzle [3].
Nevertheless, these tests showed that the temperature in the nozzle extension was too low and the run time too short to obtain good statistics in CARS and PIV measurements. Thus, to sustain higher mixture ratios and longer duration tests, it was decided to build a new combustor, water-cooled and fed with multiple injectors within the common Onera-Cnes CONFORTH project. The enhanced goal is to acquire an aero-thermal database for both the thrust chamber and the nozzle. So, about 200 thermocouples were implemented in the wall and at the face plate of the combustor, distributed along three generating lines.
A first acceptance test campaign was performed in 2010, during which the chamber was fed with gaseous oxygen and gaseous hydrogen. A new test procedure was defined in order to ignite at a specified operating point, common to all tests, and then to move to the target operating point. The combustor successfully worked in the operating domain of Mascotte: pressure ranging from 2 MPa to 6.5 MPa and mixture ratio (O/F) varying between 2 and 7. Heat fluxes for the different parts of the combustor, as well as adiabatic temperature and heat transfer coefficient for the face plate, have been deduced from temperature measurements, leading to a database which first helps to consolidate the design procedure, and later, can be used for CFD validation in the near future.

2. Experimental set-up

2.1. Description of the hardware
Several versions of the hardware have been developed and manufactured for the different items of interest in experimental research. The first one is the "thermal" version (Fig. 1a); it consists of an injection head with an instrumented sleeve (non-cooled), two ferrules, water cooled and equipped with thermocouples along three generating lines, and an axi-symmetric nozzle. In the second version (Fig. 1b), devoted to optical diagnostics, the first ferrule is replaced by a visualization module with four optical ports. The aim of the third version (Fig. 1c) is to investigate the separation of the flow in an over-expanded nozzle, in the framework of the ATAC program [3]. Figure 2 shows the instrumented hydrogen sleeve. Fourteen thermocouples are distributed on five circles among the five injectors, one central and four peripherals. These can be located on two diameters. During the acceptance tests, injectors were located on the inner diameter. This change of position allows investigating the sensibility of heat fluxes to the distance between the wall and the injector.

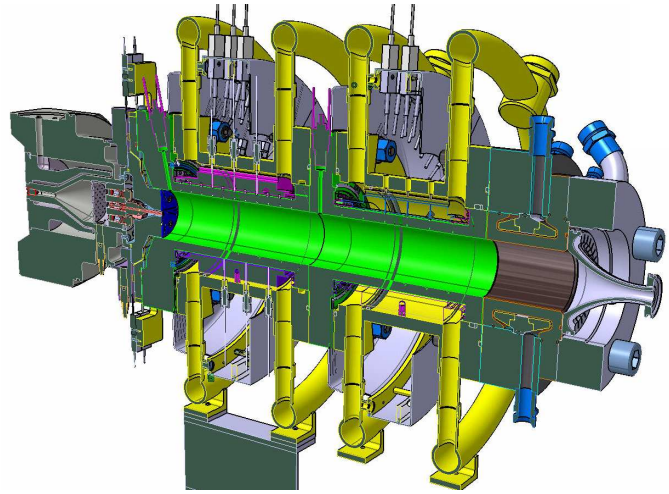

a) Thermal version: two water-cooled ferrules equipped with thermocouples for heat transfer investigations.

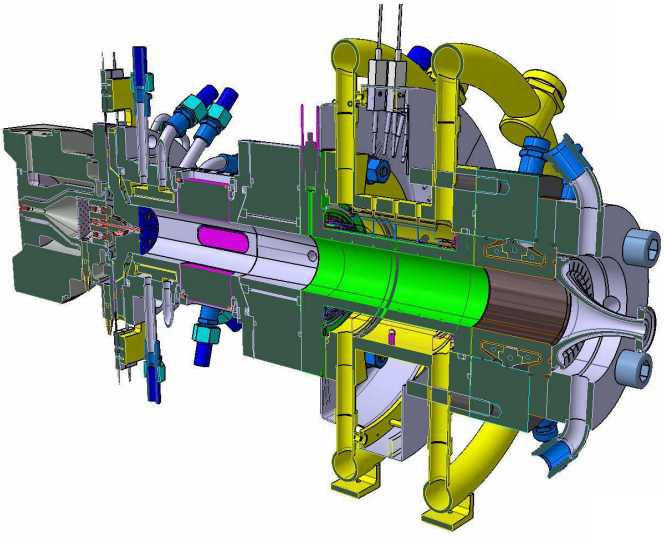

b) Visualization version: one of the ferrules replaced by a module with optical ports.

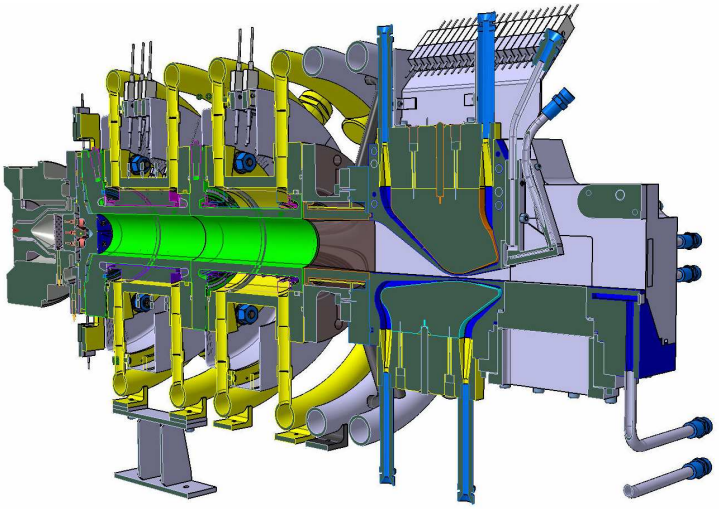

c) “ATAC” version: a 2D nozzle for investigation of flow separation.

Figure 1: The water-cooled combustion chamber.

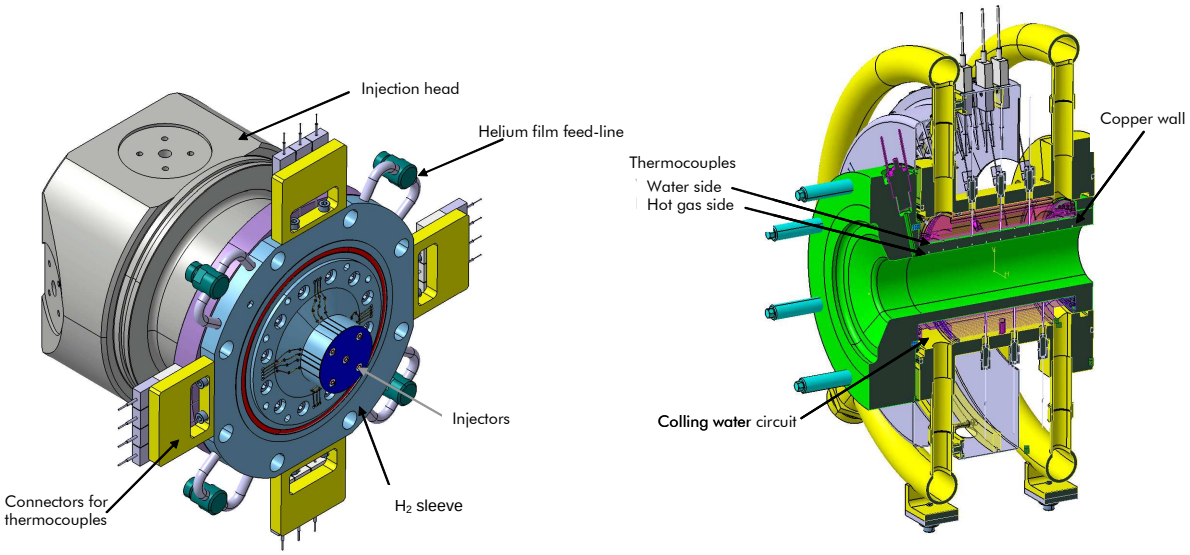

Figure 2: The instrumented hydrogen sleeve (left) and the first ferrule (right).

For long duration tests, this instrumented sleeve is replaced by a water-cooled one made of the same material than the ferrules walls.
Figure 2 also shows the first ferrule of the thermal version. The central part consists of a 10 mm thick wall, equipped with pairs of thermocouples located on both sides. It is also equipped with pressure transducers and a port hole for the torch igniter.
The inner diameter of the combustion chamber and the diameter of the nozzle throat are the same than in the previous Mascotte combustors.

2.2 Test plan

At the beginning of the acceptance test campaign, a safe start point was determined at low mixture ratio and chamber pressure of 0.7 MPa. This point was used for all the tests. The different target points were than reached by increasing simultaneously the oxygen and hydrogen mass flow rates. Figure 3 shows typical test sequences of a short duration run (left) and a long duration run (right). The steady-state is nearly the same for both: chamber pressure P = 6.6 MPa and mixture ratio O/F = 6.1. This corresponds to the highest load point reached during this test series.
The achieved operating points of the short duration tests are located in the (mixture ratio, chamber pressure) plane on Figure 4, where the expected dimensionless heat flux are represented by the color scale.

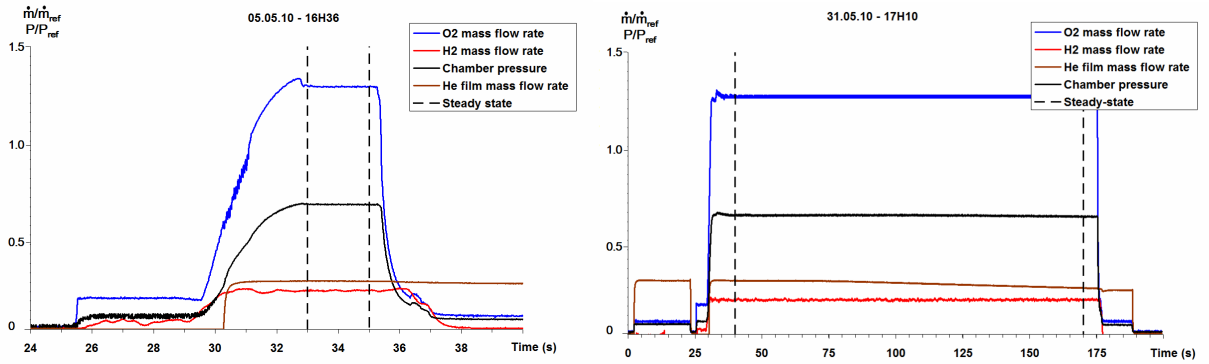

Figure 3: Typical test sequences, short duration left, and long duration right

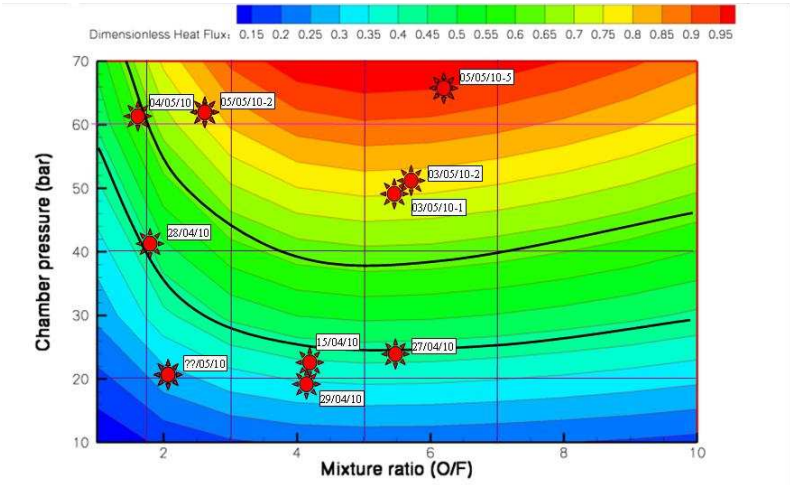

Figure 4: Achieved operating points of the acceptance test series

3. Thermal measurements, counting methods and results

One of the first goals of the acceptance tests was to validate the assumptions made on the heat fluxes during the design of the different parts of the combustion chamber. The heat flux calculation is depending on the considered part of the combustor: the ferrules or the injection head, or more exactly the hydrogen sleeve. The latter was instrumented but non-cooled during the first test series. The other parts were water cooled, so that the heat fluxes could be derived from a spatial gradient between two thermocouples located near the walls, one on the hot gas side and one on the cooling water side. The heat fluxes in the injection head were estimated from a temporal gradient by

the usual procedure of counting used in previous thermal measurements campaigns on Mascotte. This implies that the heat flux is spread in one direction only, which amounts to assume that it is homogeneous on the surface, or in other words, that the longitudinal temperature gradients are much more important than the transverse gradients. Preliminary calculations showed that this assumption was relatively well verified, even if many recirculation zones between the injectors generate flux variations on the injection plate. A more accurate determination of the heat fluxes would have been possible by application of an inverse method, but its implementation and systematic use would have been too heavy and disproportionate in the context of the acceptance campaign. To address the need of immediate use between two successive tests, specific software, based on a LabView application, was written to visualize rapidly the temperatures and the heat fluxes on the different parts of the combustor. This helped to make a decision: "go or no go" to the next hot fire test. This software includes: restitution of the measured wall temperatures (with an extrapolation from the neighbours for the off thermocouples); derivation of heat fluxes from these temperatures; animated 3D visualization of the results; archiving in data files adapted to further post processing.

3.1. Technical specification of thermal calculations software

3.1.1. Nomenclature

α	Thermal diffusivity (in [m²/s]) ($\alpha = \lambda/(\rho C_p)$) Thermal expansion coefficient (in [K^{-1}])
λ	Thermal conductivity (in [$W \cdot m^{-1} \cdot K^{-1}$])
ρ	Density (in [$kg.m^{-3}$])
τ_o	Fourier time (in [s])
φ	Surface density of flux (in [$W.m^{-2}$])
Φ	Heat flux (in [W])
C_p	Heat capacity (in [$J.kg^{-1}.K^{-1}$])
E	Effusivity (in [$J.K^{-1}.m^{-2}.s^{-1/2}$]) ($E = (\lambda \rho C_p)^{1/2}$)
T	Temperature (in [K])

TC : thermocouple
PE : water side wall
PG : gas side wall
RC : cooling water circuit

3.1.2. Functional Overview

There are four types of thermocouples (TC) on the CONFORTH combustor: TC for measuring the temperature of the water with which energy balance is made between input and output; TC for measuring heat fluxes by conduction in a semi infinite wall, i.e. the TC of the non-cooled hydrogen sleeve with some corrections and those of uncooled nozzles; TC for measuring heat fluxes in a thin wall, i.e. those of the ferrules; TC for monitoring the temperature, to which no treatment is applied.

3.1.3. Physical data needed

The hydrogen sleeve is made of Inconel. The combustion chamber consists of two ferrules for thermal measurements. Their core is made of an alloy whose thermal properties are function of temperature.

3.1.4. Heat flux calculation

Heat flux on the hydrogen sleeve

The heat flux on the sleeve is calculated by the usual procedure for a semi-infinite media [4], [5]. For capacitive heat flux meters, the heat flux is deduced from the temporal variation of the surface temperature.

$$\varphi(t) = \frac{E}{\sqrt{\pi}} \int_0^t \frac{dT}{d\tau} \frac{d\tau}{\sqrt{t-\tau}} \qquad \textbf{(1)}$$

If the physical and thermal characteristics of the material are assumed constant, the best approximation being the values corresponding to the mean temperature of the heating up phase, and if $dT/d\tau$ is constant during the time step $\Delta t = t_{n+1} - t_n$ this expression can be numerically integrated :

$$\varphi(t) = \frac{2E}{\sqrt{\pi \Delta t}} \sum_{n=1}^{N} \left\{ \left[T_n - T_{n-1} \right] \left[\left(N - n + 1 \right)^{1/2} - \left(N - n \right)^{1/2} \right] \right\} \quad \textbf{(2)}$$

However, the thermocouples are located a little bit away from the wall. So there is a phenomenon of delay and diffusion leading to an underestimation of the heat flux. The delay is given by the Fourier time: $\tau_0 = L^2/\alpha$. It is an order of magnitude smaller than the response time of a thermocouple that is around 0.1 s. The calculation method is thus valid.

Heat flux on the ferrules

There are two main methods to calculate the heat flux from temperature measurements: the first one described above, uses the temporal evolution during transient phases, and the second one, the spatial variation during the steady state [6]. The choice is determined by the Biot (Bi) number. For Bi below 0.1, one can assume that thermal equilibrium is reached in the wall, while for Bi above 0.1, the wall can be considered as a semi-infinite media. With our conditions, we can consider that the temperature in the wall is in equilibrium with respect to heat exchange. However, it is necessary to estimate the diffusion time of a temperature change, i.e. the Fourier time. For a wall thickness of 10 mm, this time is 1 s, which is large enough compared to the sampling period. This shows that during very rapid changes in temperature, the wall can be considered as a semi-infinite wall, while at steady state it behaves as a thin wall. We therefore propose to select at each time step, the maximum between the flux deduced from the temporal evolution of the surface temperature ("Laplace" method) and the flux calculated with the spatial gradient. For the "Laplace" calculation, only the hot gas side wall temperatures are used. The heat flux density per unit area deduced from the temperature gradient is given by : $\varphi = \lambda(T).\nabla T$. For the very first exploitation of the tests, only the radial component is used. If the distance between the two thermocouples is *l* and the best approximation is obtained with the thermal conductivity at the mean temperature between the hot gas side (T_{PG}) and the cooling water side (T_{PE}) , thus:

$$\varphi = \lambda((T_{PG}+T_{PE})/2) \times (T_{PG} - T_{PE})/l \quad \textbf{(3)}$$

3.2. Results for the most restrictive operating point

Figure 5 displays the temperatures measured on the first ferrule and on the hydrogen sleeve during the short test of figure 3. The heat fluxes that are deduced from those measurements are given as well. For the ferrule the fluxes calculated from the temporal and from the spatial gradients are both presented. To obtain the first one from the temporal evolution of the surface temperature (i.e. the hot gas side thermocouple), it is assumed that the wall is semi-infinite and exposed to an uniform flux. This assumption is of course realistic only in the very first moments of the run. For the latter, we consider the diffusion of heat through the wall and use the difference in temperature between the hot wall and the cold wall. This calculation is completely valid as soon as a steady-state is reached, i.e. as soon as the temperatures become stationary. Comparing the two methods allows us to reinforce the magnitude of fluxes.

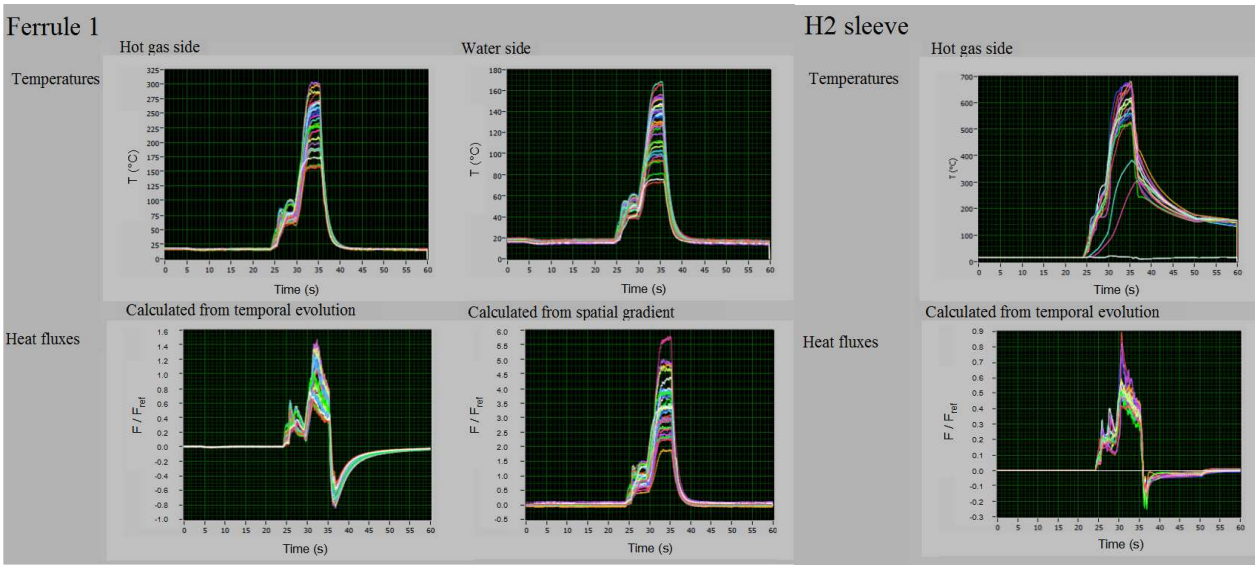

Figure 5: Temperatures and heat fluxes on the ferrule 1 and on the hydrogen sleeve (P = 6.6 MPa , O/F = 6.1)

The right part of the figure concerns the instrumented sleeve. For this, a spatial gradient type calculation is of course not possible since this part is non-cooled and there are thermocouples on hot wall side only. Figure 6 is a representation of the temperature field at several moments, obtained by symmetrising the measures of the fourteen thermocouples actually present on the face.

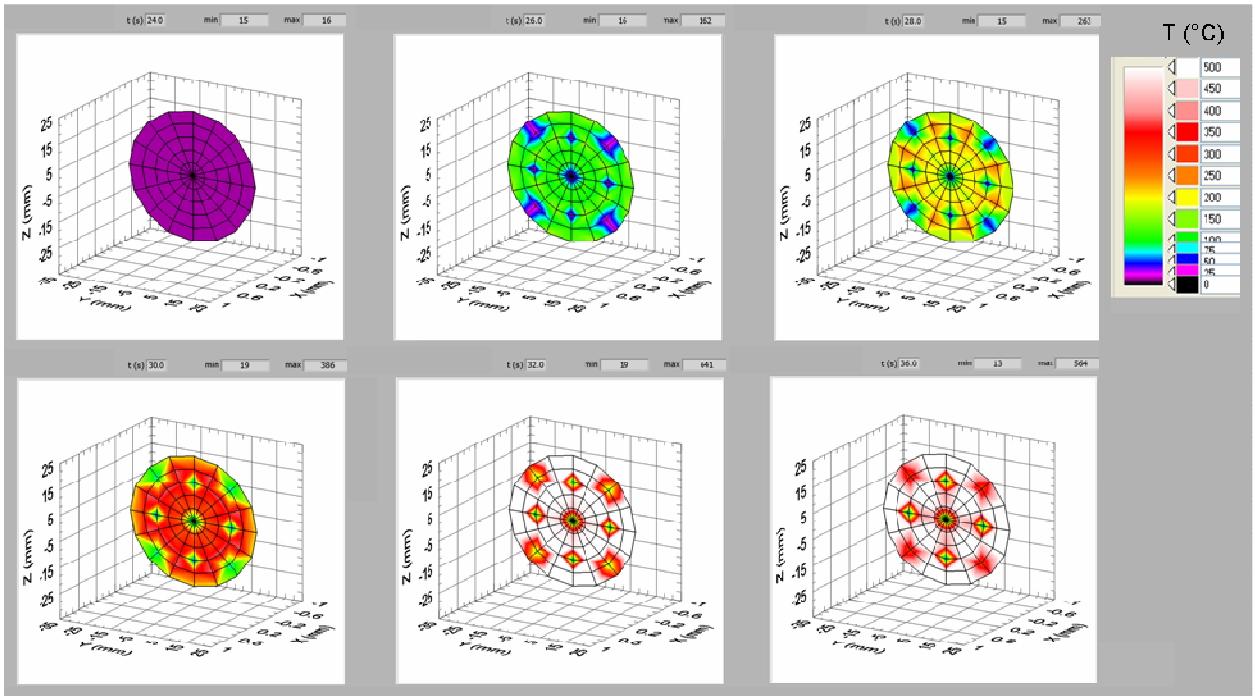

Figure 6: Temperatures on the face plate (P = 6.6 MPa , O/F = 6.1)

Figure 7 shows the temperatures measured on the hot gas side and on the cooling water side of the two ferrules during the steady state of the long duration test. It can be noticed that the trace of the injectors extends quite far from the face plate, as the temperatures begin to homogenize only at the end of the ferrule 1. This zone is located downstream of the maximum temperature, which probably corresponds to the region where the flame of the injectors hits the wall. The recorded maximum temperatures are higher than the design assumptions, but there is still some margin before reaching values that could damage the material.

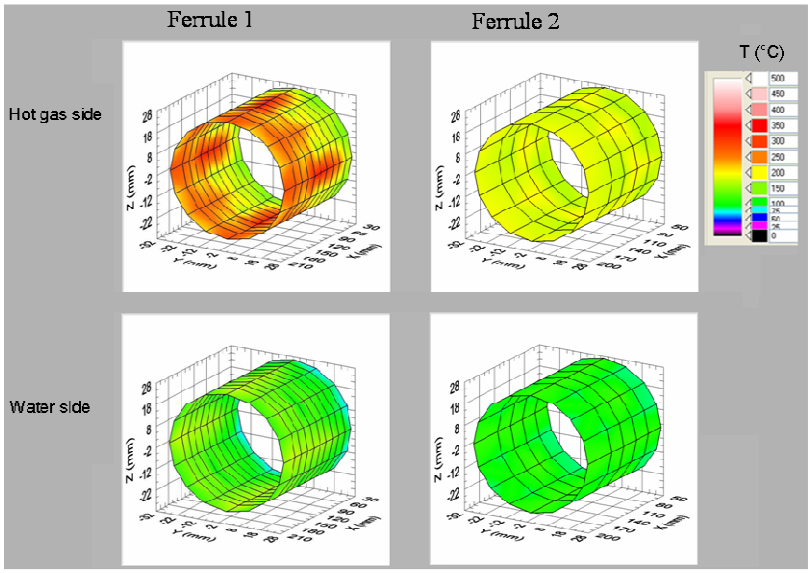

Figure 7: Temperatures of the ferrules at steady-state

Figure 8 compares the temperatures observed during the steady-sates of the short and of the long test. It is roughly the same operating point and we can see that the temperature fields are very similar.

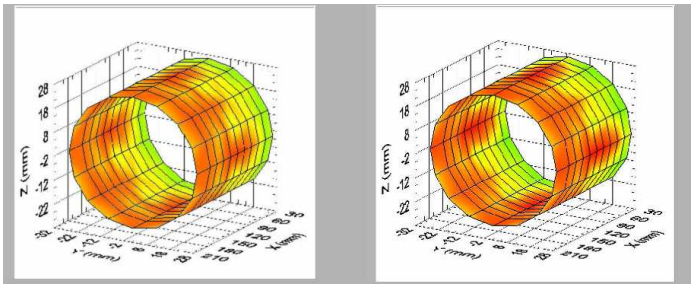

Figure 8: Temperatures of the hot gas side of ferrule 1 for a short test (left) and a long test (right)

3.2. Heat exchange characteristic parameters

Hardware design requires thermo-mechanical calculations. For these, the heat flux φ applied as boundary condition is classically described by two characteristic parameters: an exchange coefficient h, obtained from the Bartz correlation, and the adiabatic wall temperature T_a , often linked to the stagnation temperature of the flow. The relationship between these quantities is: $\varphi = h\ (T_a - T_w)$ where T_w is the wall temperature. When the flow is stabilized, h and T_a are constant so that the flux depends linearly on the wall temperature. This property can be used to evaluate these two parameters.
Figure 9 displays the flux versus the temperature for two of the thermocouples on the outer row of the sleeve. A straight line can be fitted on the part of this curve corresponding to the steady-state with a reasonable regression coefficient for the TC in front of the injector. For the other one, the discrepancies reveal a more unsteady flow due to the large recirculation in this region. Nevertheless, the heat exchange coefficient h is given by the inverse of the slope and the adiabatic temperature by the intercept divided by h. The uncertainty of this method was less than 10% for the determination of the adiabatic temperature, but it could reach 30% for h, depending on the operating point and on the location of the thermocouple. This treatment applied to all the TC are summerized figure 10.

In conclusion, this operation has demonstrated the feasibility of determining the exchange coefficients and adiabatic wall temperatures. However, for some measurement positions, principally near the injectors, local fluctuations of the flow lead to somewhat inaccurate values. It remains that the obtained exchange coefficients are consistent and higher than the values used for the design.
The adiabatic temperatures, in contrast, are much lower than those provided by a CFD computation prior to the thermo-mechanical sizing, and are relatively independent of the operating point. We recall that they were in an interval [1000 K 2400 K].
It therefore seems possible to think that cooling the wall of the ferrules has a definite influence on the stratification of the flow on the sleeve.

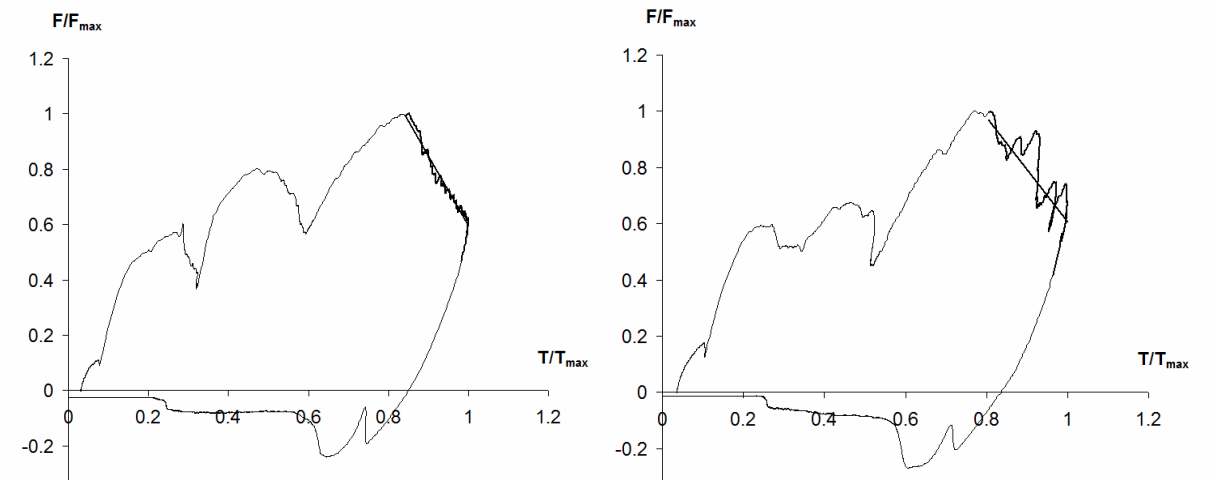

Figure 9: Heat flux versus temperature on the hydrogen sleeve in front of injector (left) or between 2 injectors (right)

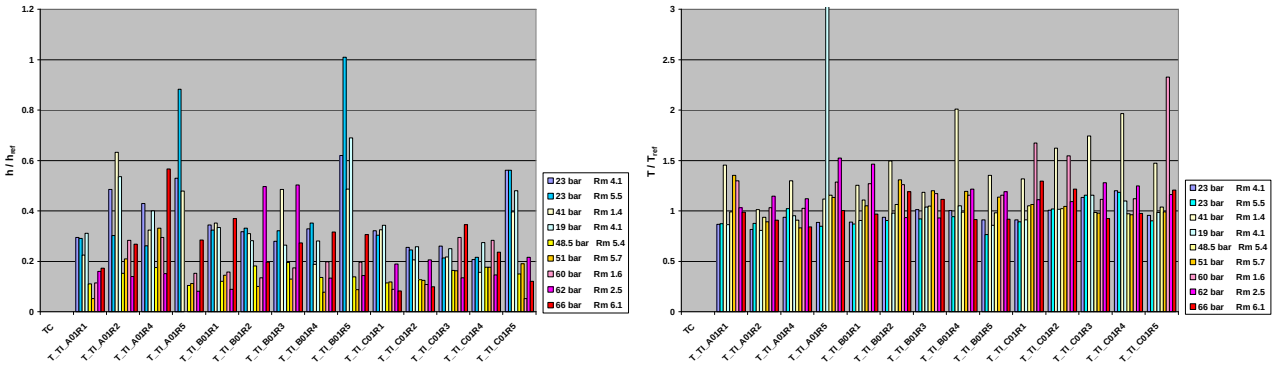

Figure 10: synthesis of heat exchange coefficient (left) and adiabatic wall temperature (right)

4. Conclusion

A new water-cooled combustion chamber adapted to the cryogenic bench Mascotte was developed by Onera in partnership with the CNES. The modular approach of this new experimental device allows the thermal characterization, optical diagnostic and the analysis of the unsticking of jet in nozzle for close conditions of functioning (multi-injection, high-pressure and high mixture ratio) of those met in combustion chambers of engines rocket. A first campaign performed with multiple injection of Gox / GH2 was realized. It has explored all the domain of planned functioning. A quasi instantaneous exploitation of the temperatures measurements has allowed to validate the chosen criteria of sizing based on thermal exchange coefficient and wall adiabatic temperature, even though some discrepancies were found due to different thermal stratification from that used initially . The good results of this campaign allow pursuing with confidence the following activities consisting in multiple Lox / GH2 injection and combustion characterisation and visualization.

References

[1] Vingert, L., Habiballah, M., and Vuillermoz, P. 2002. Upgrading of the Mascotte cryogenic test bench to the LOX/Methane combustion studies. In: 4th *Int. Conf. on Launcher Technology*.

[2] F. Richecoeur, S. Ducruix, P. Scouflaire and S. Candel 2008 Experimental investigation of high-frequency combustion instabilities in liquid rocket engine *Acta Astronautica*, 62, 18-27.

[3] Ordonneau, G., Grisch, F., Hervat, P., Reijasse, P. and Vingert, L. 2005. Experimental characterisation of reactive flows in the separation region of an over-expanded two-dimensional nozzle. In: 6th *Int. Conf. on Launcher Technology*.

[4] Guernigou J., Indrigo C., Maisonneuve Y., Mentré P.G. 1980. Mise au point de fluxmètres à température superficielle. *La Recherche Aérospatiale* n°1980-3, 159-168

[5] Vingert, L. and Mayer, W. 2000. Common generic injector, definition, operating conditions and preliminary experiments. In: 6th *French-German Colloquium on Research in Liquid Rocket Propulsion*.

[6] Susslov, D., Woshnak, A., Greuel, D. and Oschwald, M. 2005. Measurement techniques for investigation of heat transfer processes at European research and technology test facility P8. In: *1st EUCASS*